NUMERICAL INVESTIGATION OF DIPOLE-EXCHANGE SPIN EXCITATIONS IN NICKEL NANOWIRES

Zavislyak I. V., Popov M. A.
National Taras Shevchenko University of Kyiv
64 Volodymyrska Str., Kyiv, 01033, Ukraine
Ph.: +38(044) 521-32-37; e-mail: maxim_popov@univ.kiev.ua

Abstract — Numerical investigation of static and dynamic properties of Ni cylinder nanowire of finite height was conducted. Frequencies of two lowest even and odd dipole-exchange spin modes as a function of applied bias magnetic field were plotted.

I. Introduction

In recent years a method of nanosize arrays of metal (Co, Ni, Fe, permalloy) wires or particles with other shapes fabrication has been elaborated and improved and static properties of such nanoobjects are being studied using various techniques [1-5]. Dynamic properties of arrays of nanowires such as excitation of coherent spin waves also being studied experimentally using Brillouin light scattering [6] and ferromagnetic resonance (FMR) [7].

From the theoretical point of view, spin waves in longitudinally magnetized cylindrical wires (taking into account exchange) were described in [8] while for perpendicular magnetization spin-wave spectrum has been calculated only in magnetostatic approximation [9] or using approximation of perturbation theory [10]. Another constriction of above-mentioned theories is that they consider a ferromagnetic cylinder as infinite one. Thus, the non-uniformity of internal magnetic field [11] is not taken into account. While for most nanowires with aspect ratio in order of 10 this is a rather justified approximation, for others it will lead to a fundamental mistake.

Therefore, at present, the main approaches to spin excitations investigation are various numerical micromagnetic methods [1, 3, 5, 12].

II. Main Part

In our calculations we will use public domain OOMMF micromagnetic solver [12-14]. The subject under investigation is isolated cylindrical Ni nanowire with diameter $d = 20$ nm and height $h = 176$ nm. We have taken the following magnetic parameters for Ni: $4\pi M_S$ = 6000 G, g = 2.18, exchange stiffness A = $8 \cdot 10^{-7}$ erg/cm, anisotropy was neglected. Therefore, the Ni exchange length $l_{ex} = \sqrt{A / 2\pi M_S^2}$ is 7.5 nm. For trustworthy results any dimension of cell used in calculations should not exceed the exchange length. Our goal was to investigate static and dynamic properties of Ni cylinder under transversal magnetization.

The following notation is used in paragraphs below: axis z is assumed to be parallel to the cylinder axis, while axes x and y are perpendicular. Due to rotational symmetry we are free to align x along the applied external magnetic field.

a. Static properties. Hysteresis loop.

At the beginning, hysteresis behavior of Ni cylinder was analyzed by applying the static magnetic field perpendicularly to the cylinder axis. The magnetic field was changed step-by-step and the total magnetic energy was minimized with respect to 3D magnetization orientation in each cell. Cell size was chosen to be 2 nm, which is small enough to correctly account exchange interaction. Each time a minimum energy state, calculated at previous step, was taken as an initial for next step, and thus a full hysteresis loop was obtained. Spatially averaged magnetization vector M_x in the x direction, normalized by the saturation magnetization M_S is shown on Fig. 1.

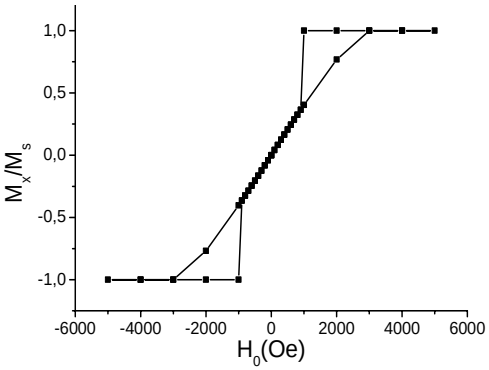

Fig. 1. Hysteresis loop for transversally magnetized Ni cylinder

Magnetization distribution shows that internal magnetic field is most non-uniform near the edges of cylinder, while in the middle it is nearly constant, as one can expect. However at a large bias field all magnetization vectors are aligned with external magnetic field.

One can see that full saturation is achieved when $|H_0| = 2\pi M_S$ =3000 Oe, just as it should be, because demagnetizing factor $N_x \approx 1/2$. It is interesting, that fully saturated state retains only till $|H_0| > 1000$ Oe, below it magnetization scales linearly with applied field. We believe that such hysteresis behavior is dictated by the absence of lattice defects and energy dissipation in mathematical model that, otherwise, would lead to more classical hysteresis appearance.

b. Dynamic properties. Spectrum of dipole-exchange spin excitations.

Starting from the minimum energy state, calculated in previous section (thus the non-uniform internal magnetic field was accounted for), the magnetization was excited by a short, strong, spatially uniform (SU) or antisymmetric with respect to z (AS) magnetic field pulse with Gaussian time dependence. The field direction in pulse was perpendicular to the static bias field, namely parallel to z direction. Pulse amplitude was 100 Oe, large enough to excite normal spin-wave modes, but much less then bias field. After the field pulse the evolution of 3D magnetization was calculated by micromagnetic simulations based on the numerical integration of the Landau-Lifshitz-Gilbert equation of motion with damping parameter α =0.01, which is reasonable value for metallic ferromagnets. Further, the magnetization state $\vec{M}(\vec{r}, t)$ was captured at uniform time intervals $t_i = i \cdot \Delta t$, $i = 1..N$. Cell size was chosen 4 nm in order to reduce computation time.

2009 19th Int. Crimean Conference "Microwave & Telecommunication Technology" (CriMiCo'2009). 14-18 September, Sevastopol, Crimea, Ukraine
 ISBN: 978-966-335-244-2. IEEE Catalog Number: CFP09788

Hence, for each point $\vec{r}_j$ in ferromagnetic, a time series of the magnetization was recorded. Typical simulated $M_z(\vec{r}_j,t)$ dependence for SU pulse is shown on Fig. 2.

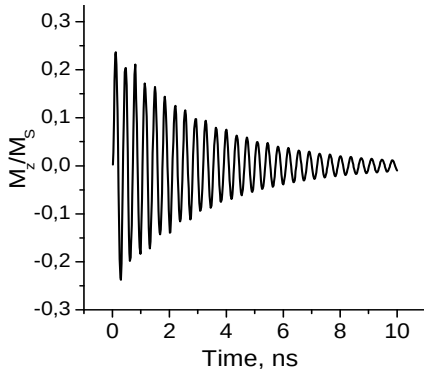

Fig. 2. Time dependence of local transversal magnetization component. Applied field H=3000 Oe

For each applied magnetic field the local power spectrum of magnetization was obtained by discrete Fourier transformation of transversal magnetization.

$$S_z(\vec{r}_j,k\cdot\Delta f)=\left|\frac{1}{\sqrt{N}}\sum_{i=1}^{N}M_z(\vec{r}_j,i\cdot\Delta t)e^{\frac{-i2\pi(k-1)(i-1)}{N}}\right|^2$$

Here $\Delta f=1/T$, where $T=N\Delta t$ - is total simulation time. To obtain an overall power spectrum, all local spectra were summed over $\vec{r}_j$ [14]:

$$S_z(k\cdot\Delta f)=\sum_j S_z(\vec{r}_j,k\cdot\Delta f)$$

Our goal was to investigate spectrum of dipole-exchange spin excitations up to 50 GHz. Therefore, the full width at half maximum (FWHM) of Gaussian pulse was chosen 33 ps, which should provide excitation of modes with frequencies up to at least 60 GHz. Time intervals were Δt chosen according to Kotelnikov theorem $\Delta t=1/(2F_{\max})$, as Δt =20 ps ($F_{\max}$ =25 GHz) for low magnetic fields ($H_0\le 8000$ Oe) and Δt =15 ps ($F_{\max}$ =33 GHz) for higher fields. Total simulation time was taken T=(4…10) ns for different magnetic fields, hence frequency resolution was Δf = (100…250) MHz.

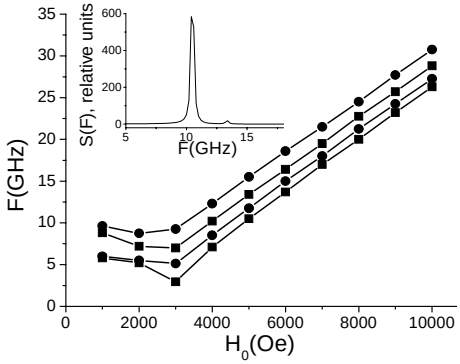

Fig. 3. Frequency vs. field dependence for transversally magnetized Ni nanowire

A typical spectrum for bias field H_0 =5000 Oe and SU pulse is shown on the inset of Fig. 3. Two distinct peaks are clearly visible. Frequencies of these peaks derived for each bias magnetic field for SU (squares) and AS (circles) excitations are depicted on Fig. 3. One can see a typical FMR behavior: in unsaturated region (H_0 <3000 Oe) frequency decreases with increasing magnetic field, while in saturation region increases almost linearly.

Note, that when applied magnetic pulse was spatially uniform, only modes with even longitudinal (along the axis of wire) indices were excited. It is justified by spatial magnetization distribution at resonant frequencies, according to which lower frequency mode should be designated with n=0, while the higher one — n=2. On the contrary, in AS case modes with n=1 (lower frequency) and n=3 (higher one) were excited.

III. Conclusions

In summary, we have performed numerical computations of static magnetization distribution in transversally magnetized Ni nanocylinders of finite height. As a result, a theoretical hysteresis loop was built and its properties briefly discussed.

After that, dynamic micromagnetic calculations of spin excitations spectrum in transversally magnetized Ni nanocylinders, i.e. situation for which analytical calculations are not feasible, were conducted. Non-uniform internal field was taking into account by using previously calculated static magnetization as an initial state. FWHM of exciting Gaussian pulse, total simulation time and sampling intervals were chosen appropriate for investigation of spin excitations spectrum in (0…33) GHz frequency range with resolution not worse then 250 MHz. The obtained spectrum shows four distinct peaks which were identified as perpendicular standing modes with lowest even and odd indices.

IV. References

[1] *Martin J. I., Nogues J., Liu K. et al*. Ordered magnetic nanostructures: fabrication and properties. JMMM, 2003, 256, p. 449 — 501.

[2] *Kodama R. H.* Magnetic nanoparticles. JMMM, 1999, 200, p. 359 — 372

[3] *Cowburn R. P.* Property variation with shape in magnetic nanoelements. J. Phys. D, 2000, 33, p. R1 — R16.

[4] *Henry Y., Ounadjela K., Piraux L. et al.* Magnetic anisotropy and domain patterns in electrodeposited cobalt nanowires. Eur. Phys. J. B, 2001, 20, p. 35 — 54.

[5] *Nielsch K., Hertel R., Wehrspohn R. B. et al.* Switching Behavior of Single Nanowires Inside Dense Nickel Nanowire Arrays. IEEE Trans. on Mag., 2002, 38, p. 2571 — 2573.

[6] *Gubbiotti G., Kazakova O., Carlotti G. et al.* Spin-Wave Spectra in Nanometric Elliptical Dots Arrays. IEEE Trans. on Mag., 2003, 39, p. 2750 — 2752.

[7] *Goglio G., Pignard S., Radulescu A. et al.* Microwave properties of metallic nanowires Appl. Phys. Lett., 1999, 75, 1769 —1771.

[8] *Arias R., Mills D. L.* Theory of spin excitations and the microwave response of cylindrical ferromagnetic nanowires. Phys. Rev. B, 2001, 63, 134439.

[9] *Roussigne Y., Moch P.* Spin waves in stripes submitted to a perpendicular applied field. J. Phys.: Condens. Matter, 2005, 17, p. 1645 — 1652

[10] *Tartakovskaya E. V.* Quantized spin-wave modes in long cylindrical ferromagnetic nanowires in a transverse external magnetic field. Phys.Rev. B, 2005, 71, 180404.

[11] *Joseph R. I., Schloemann E.* Demagnetizing field in nonellipsoidal bodies. J. Appl. Phys. 1965, 36, p. 1579 — 1593.

[12] *Donahue M. J., Porter D. G.*. OOMMF User's Guide, Version 1.0, Interagency Report NISTIR 6376, National Institute of Standards and Technology, Gaithersburg, MD (Sept 1999).

[13] *Jung S., Ketterson J. B., Chandrasekhar V.* Micromagnetic calculations of ferromagnetic resonance in submicron ferromagnetic particles Phys. Rev. B,2002, 66, 132405.

[14] *McMichael R. D., Stiles M. D.* Magnetic normal modes of nanoelements. J. Appl. Phys., 2005, 97, 10J901.